

Validation of neutronic models and calculation systems by means of experimental results in the IPEN/MB-01 reactor



Adimir dos Santos^{a,*}, Carlos R. Grant^b, Paulo de Tarso D. Siqueira^a, Ariel E. Tarazaga^b, Graciete Simões de Andrade e Silva^a, Claudia M. Barberis^b

^a Instituto de Pesquisas Energéticas e Nucleares (IPEN-CNEN/SP), Av. Prof. Lineu Prestes, 2242, Cidade Universitária, São Paulo, SP 05508-000, Brazil

^b Comisión Nacional de Energía Atómica (CNEA), Gerencia de Área Energía Nuclear (GAEN), Centro Atómico Constituyentes (CAC), Avenida General Paz 1499, 1650 San Martín, Provincia de Buenos Aires, Argentina

ARTICLE INFO

Article history:

Received 28 December 2012

Accepted 23 April 2013

Available online 22 May 2013

Keywords:

IRPhE

ICSBEP

HUEMUL

PUMA

IPEN/MB-01

ABSTRACT

In the year 2008 the National Atomic Energy Commission (CNEA) of Argentina, and the Brazilian Institute of Energetic and Nuclear Research (IPEN-CNEN/SP), under the framework of the Nuclear Energy Argentine-Brazilian Agreement (COBEN), among other projects, included “Validation and Verification of Calculation Methods used for Research and Experimental Reactors”. At that time, it was established that the validation was to be performed with models implemented in the deterministic codes HUEMUL and PUMA (respectively, cell and reactor codes) developed by CNEA and those implemented in MCNP5. The necessary benchmark data for these validations would correspond to the theoretical-experimental reference cases elaborated in the research reactor IPEN/MB-01 located in the city of São Paulo, Brazil. These benchmarks were previously evaluated and approved for publications in the ICSBEP and IRPhE handbooks. The staff of the Nuclear Design and Analysis Division of the Reactor and Nuclear Power Plant Study Department (ERC) of CNEA, from the Argentine side, modeled and performed several calculations with both deterministic (HUEMUL-PUMA) and probabilistic (MCNP5) methods of a great number of physical situations of the reactor, which previously have been studied experimentally and modeled by members of the Nuclear Engineering Center of IPEN, whose results were extensively provided to CNEA. The analyses reveal the great performances of ENDF/B-VII.0 in conjunction with MCNP5 and the HUEMUL and PUMA codes in all benchmark applications.

© 2013 Elsevier Ltd. All rights reserved.

1. Introduction

This paper is produced by the Research Reactors and Nuclear Power Plants Studies Department (ERC) of the Argentine National Atomic Energy Commission (CNEA), and the Nuclear Engineering Center (CEN) of the Brazilian Institute of Nuclear and Energetic Research (IPEN-CNEN/SP) under the framework of the Bi-National Commission of Nuclear Energy (COBEN), created in Buenos Aires in February 2008. A meeting of 160 researchers was organized in Foz do Iguaçu (Brazil), called “Argentina & Brazil Seminar for Nuclear Cooperation”. This paper is the final result of one of the projects proposed in that seminar, entitled “Validation and Verification of Calculation Methods used for Research and Experimental

Reactors”. The benchmarks selected for the computer code and associated library validations comprise a series of integral and differential parameters which are of interest in the reactor physics field. They have been all designed and executed in the IPEN/MB-01 research reactor facility and they have already been evaluated, approved, and published in the ICSBEP (International Criticality Safety Benchmark Evaluation Project) (Briggs, 2012a) and by IRPhE (International Reactor Physics Experiments) handbooks (Briggs, 2012b). These benchmarks are: criticality safety benchmarks including plenty of reactor core configurations, isothermal experiments which aim to quantify the error in the calculation of the isothermal reactivity coefficients, effective delayed neutron parameters which are quantities very important to infer the reactivity after a reactor perturbation and relative fission density distributions, which also are very important quantities for the determination of peaking power factors in nuclear reactors. These benchmarks are very important in practical applications and provide sufficient subsidies for establishing possible bias and margins of uncertainties in the computer codes and associated nuclear data libraries.

* Corresponding author. Address: Instituto de Pesquisas Energéticas e Nucleares – IPEN/CNEN-SP, Centro de Engenharia Nuclear (CEN), Av. Prof. Lineu Prestes, 2242, 05508-000 – Cidade Universitária, São Paulo, SP, Brazil. Fax: +55 11 3133 9423.

E-mail addresses: asantos@ipen.br (A. dos Santos), grant@cnea.gov.ar (C.R. Grant), ptsiquei@ipen.br (Paulo de Tarso D. Siqueira), tarazaga@cnea.gov.ar (A.E. Tarazaga), gsasilva@ipen.br (Graciete Simões de Andrade e Silva), barberis@cnea.gov.ar (C.M. Barberis).

The Argentine side performed calculations with the deterministic models (HUEMUL (Grant, 2012) – PUMA (Grant, 2011); cell and reactor codes, respectively) and probabilistic methods (MCNP5 (X-5 Monte Carlo Team, 2003)) by modeling a great number of physical situations of the reactor, which had been previously studied and modeled by IPEN.

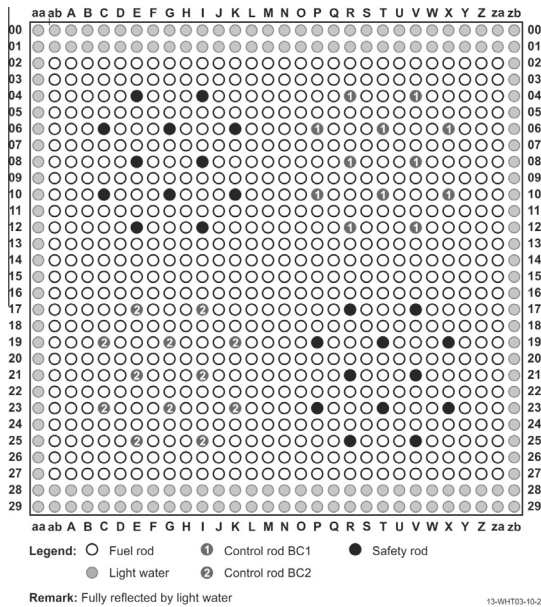


Fig. 1. Detailed scheme of the core. White positions correspond to fuel rods that can be occupied by other elements such as burnable poison rods or no rod (only water). Red positions correspond to safety rods (water when withdrawn). Yellow and blue positions correspond to absorber elements of control banks BC1 and BC2 (water when withdrawn), respectively. Black positions are water; here acting as reflector. (For interpretation of the references to color in this figure legend, the reader is referred to the web version of this article.)

HUEMUL is a 2D collision probability code in general geometry for cell and multiple cell calculations. It allows the representation of lattices with elements which can have rectilinear or curved boundaries and it is provided with all models to perform neutron cell calculations such as library management, resonance self-shielding calculations and transmutation evaluations.

PUMA is a 3D diffusion code for reactor calculation for fuel management, space kinetics and power cycle simulation. It is widely used in all nuclear installations in Argentina.

Next section contains a short description of the IPEN/MB-01 reactor and experiments. Section 3 shows the benchmark problems and the description of the experiments. Section 4 shows the results of the deterministic and stochastic codes.

2. Description of the IPEN/MB-01 research reactor facility

The complete description of the IPEN/MB-01 reactor can be found in references Dos Santos et al. (2012a–2012j). Here just some highlights will be shown in order to give some insight into the benchmark models used in the theoretical analysis. The IPEN/MB-01 research reactor facility is a critical zero power facility specially designed to measure a great variety of parameters of reactor physics to be used as benchmarks for the evaluation of calculation methods and related nuclear data libraries. It is located in São Paulo, Brazil, and it reached its first criticality in 1988. Since then, it has been used for basic research in reactor physics and for education purposes. Its core consists of a rectangular arrangement of 28 by 26 fuel rods of UO_2 enriched at 4.3486% (in weight), and a stainless steel (SS-304) cladding, immersed in a demineralized light water tank. The maximum allowed operation power is 100 W. The reactor control is performed by means of two rod banks diagonally opposed each other; the other two diagonal zones are occupied by the safety rod banks. Each control bank is composed by 12 absorber rods of Ag–In–Cd, and each safety bank by 12 absorber rods of B_4C . The control and safety bank's location in the x – y plane can be seen in Fig. 1. The reactor lattice is rectangular with a 1.5 cm

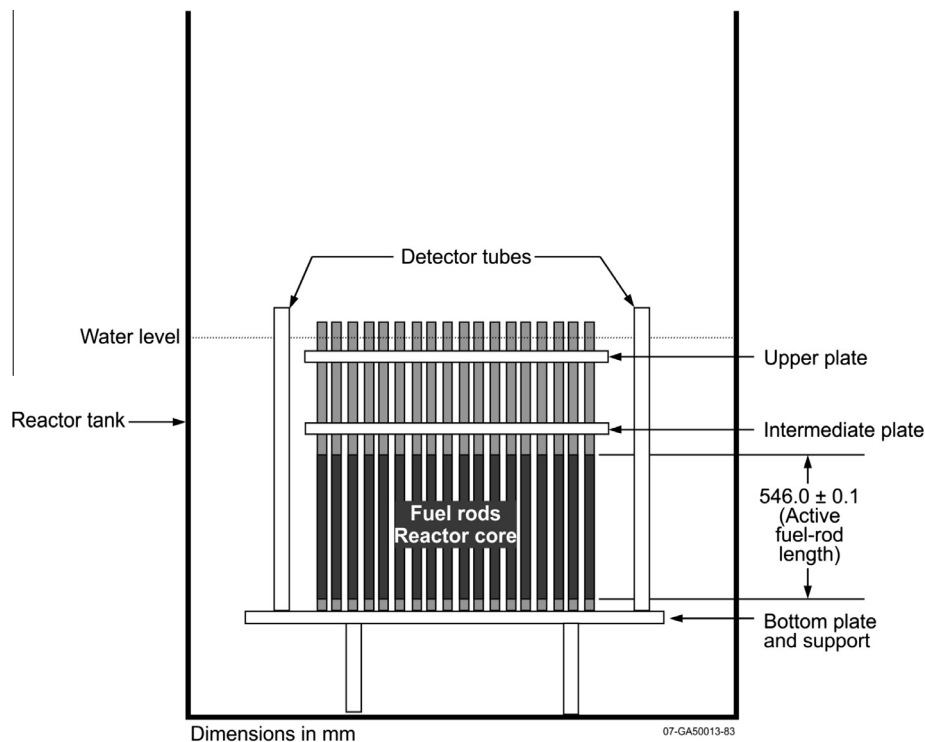


Fig. 2. Vertical scheme of the core tank.

pitch and it was chosen to optimize the fuel to moderator relation (close to the maximum value of k_{∞}). During normal operation the safety banks are totally withdrawn and their guide tubes are filled with water. In their totally withdrawn position (nearly 35 cm from the top of the fuel active length), the safety banks do not impose any appreciable reactivity effect and therefore they can be neglected in the whole analysis performed in this work. Figs. 1 and 2 show, respectively, some details for the x - y plane and z axis of the reactor core. The IPEN/MB-01 reactor design is especially versatile to allow a great variety of geometries. Fuel rods can be disposed describing different core shapes and can be removed from any part of the rectangular arrangement. Therefore strange elements can also be introduced into the reactor such as fuel rods with burnable poisons. Reflector changes can also be done. With exception to the isothermal experiment, in all other cases presented here, safety and control rod positions remain at the same withdrawn level. The IPEN/MB-01 reactor is characterized with a sufficient detail in chemical and isotopic material composition as well as in their geometric characterization to produce international reference cases.

All data provided by the sources of references Dos Santos et al. (2012a–2012j), together with their corresponding uncertainties in geometric dimensions and material compositions, have been used in input data of HUEMUL, PUMA and MCNP5. These references describe a series of simplifications in order to arrive to a theoretical-experimental benchmark model for the theoretical analysis.

3. Description of the benchmark problems

3.1. Experiment descriptions

The reactor physics experiments selected to serve as benchmark problems for the computer codes and associated nuclear data libraries were all evaluated, approved and published at the IRPhE handbook (Briggs, 2012b). These experiments include several kinds of classical reactor physics problems and were all designed, executed and evaluated at IPEN. Due to their complexity and importance for the validation process performed in this work, these experiments will be described in a more detailed fashion in the following sub-sections.

3.1.1. Critical configurations

The critical experiments selected for the computer codes and associated nuclear data library validations are all available in the ICSBEP handbook and they comprise an extensive set of configurations. The full report (Grant et al., 2011) that outcomes from the Brazil-Argentina cooperation contains the analysis of 56 critical configurations, but in this paper only some of them will be shown for the sake of brevity. The 56 critical configurations were all calculated by HUEMUL-PUMA and from them only a subset was selected for the MCNP calculations; this subset is the one that will be shown here. References Dos Santos et al. (2012a–2012j) show extensive descriptions of all configurations analyzed in this paper.

3.1.2. The isothermal temperature coefficient experiment

The object of this experiment is to address a specific need to establish a reactor response that is sensitive to the ^{235}U cross section shape below 5.0×10^{-3} eV. This experiment exploits the very precise control bank critical position system (Dos Santos et al., 1999) of the IPEN/MB-01 reactor. The control bank system characteristics of the IPEN/MB-01 reactor can be classified as one of the most accurate of such systems that have ever been built anywhere in the world. Basically, the experiment consists of a sequence of heating steps of the moderator water tank, followed by a period when the heater is turned off to let the system reach thermal

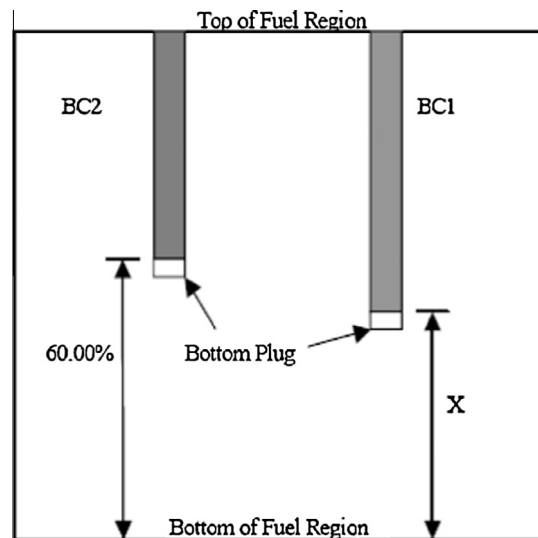


Fig. 3. Schematic vertical representation of control rod bank positions during the experiment performed to evaluate the temperature reactivity coefficient. "X" is the adjustable variable to reach criticality as a function of temperature.

equilibrium. The basic experimental data is a set of critical control bank positions as a function of temperature.

During the experiment, both of the safety banks were kept completely in the withdrawn position, and there is no need to consider them in the analyses. The reactor was kept critical during the whole experiment. The BC2 control bank was kept fixed at the 60.00% withdrawn position, and the fine criticality control was achieved by the automatic control system continuously positioning the BC1 control bank around the true position of criticality. Fig. 3 shows, schematically, the control bank configuration for the experiment. The reference level for the withdrawn position is the bottom of the fuel region, and the uppermost position (100 % withdrawn) is the top of the fuel region. The variable X represents a generic critical withdrawn position. The power level was kept at 1 W throughout the experiment.

3.1.3. The fission density distribution experiment

The purpose of this experiment was to determine the relative fission density distribution in the core of the IPEN/MB-01 reactor. The methodology is based on the proportionality between the gamma activity emitted by the radioactive decay of the fission products and the fission density in the fuel pellets (Kobayashi et al., 1978). The fission products are, in general, radioactive and they decay either by the emission of β and/or γ . The final gamma emission spectrum is a complex function of the irradiation history and the decay period. However the aggregate behavior after the irradiation can be obtained experimentally and utilized to infer the fission density distribution of the fuel rod. If the gamma activity is determined soon after the irradiation it can be affirmed that the measured radiation is proportional to the fission distribution. The measurements consider only the gammas with energy above 0.6 MeV (Myiosh et al., 1993) mainly for the exclusion of the gammas emitted by ^{239}U and ^{239}Np (Reus and Westmeier, 1983). These nuclides arise from a (n, γ) reaction in ^{238}U that occurs mainly in the epithermal region of the neutron spectra, and it is not proportional to the local fission density. The measurements were performed by gamma scanning equipment. This equipment is composed of lead shieldings and collimators, a system for the accommodation of the fuel rod, and a gamma detector. The fuel rod scanning is performed stepwise by a step motor unit and a relative position indicator. A maximum of two experimental fuel rods were measured in the scanning equipment for each operation of the reactor.

$$\alpha_{\text{isoerror}} = \frac{k_{\text{eff}}(T_1) - k_{\text{eff}}(T_2)}{k_{\text{eff}}(T_1)k_{\text{eff}}(T_2)\Delta T} \quad (1)$$

where T_1 is 20 °C, T_2 is 80 °C, k_{eff} is the calculated critical multiplication factor at the temperatures T_1 or T_2 , and ΔT is equal to $T_2 - T_1$.

The benchmark values for the relative fission density distribution are given in the IRPhE handbook. The quantities to be calculated are expressed mathematically as:

$$RFD = \frac{1}{F} \int_E dE' \int_{4\pi} d\Omega' \int_V dr^3 \Sigma_f(\vec{r}, E') \varphi(\vec{r}, \hat{\Omega}', E') \quad (2)$$

where RFD represents the relative fission density, $\Sigma_f(\vec{r}, E)$ is the macroscopic fission cross section of the fuel region at position \vec{r} and neutron energy E , $\varphi(\vec{r}, \hat{\Omega}, E)$ is the neutron flux at position \vec{r} , neutron direction $\hat{\Omega}$ and neutron energy E , and F is the fission density at the reference position. The fuel region is divided into a series of cylinders whose radius is the pellet radius and its height is equal to 1.0 cm. The tri-dimensional space integral of Eq. (2) is performed only inside each one of these cylinders. The axial position of the center of the first cylinder is equal to 2.5 cm and that for the following others are located at ever two cm interval, up to 525 mm considering all axial distances from the bottom of the active length of the fuel pellet stack. The reference position is located at the axial distance of 225 mm from the bottom of the active length of the fuel rod M14. This position was chosen because M14 is one of the central fuel rods and the fission density at its axial distance of 225 mm in the final set of measurements is very close to the maximum value. The terminology M15, M27, and so on, refer to the fuel rod location in the x - y plane shown in Fig. 1. Due to its very large volume of data, only a few representative fuel rod positions will be reproduced here. The theoretical analyses consider positions M15, M27, ab27, and B24 (see Fig. 1), which represent several extreme cases. M15 is a central position, M27 is a position in the core-reflector interface, ab27 is at the corner, and B24 is very close to the control bank. Table 1 summarizes the benchmark values for the relative fission density considered for the MCNP5 calculations. Additional comparisons for positions I16, ab02, Q11, ab10, N09, M02, N20, N27, T15, Y06, J18, and ab19 will be considered in the case of HUEMUL-PUMA codes.

Table 1
Relative Fission Density Distributions for Positions M15, M27, ab27 and B24. The data are normalized to the axial distance of 225 mm of fuel rod M14.

Axial distance (mm)	POSITION M15		POSITION M27		POSITION ab27		POSITION B24	
	RFD	UNCERT 1(σ)	RFD	UNCERT 1(σ)	RFD	UNCERT 1(σ)	RFD	UNCERT 1(σ)
25	0.5371	0.0041	0.3798	0.0034	0.2245	0.0045	0.2122	0.0047
45	0.6040	0.0045	0.4268	0.0037	0.2572	0.0050	0.2388	0.0052
65	0.6782	0.0048	0.4894	0.0041	0.2891	0.0055	0.2690	0.0057
85	0.7555	0.0052	0.5414	0.0045	0.3232	0.0060	0.2998	0.0062
105	0.8261	0.0055	0.5875	0.0048	0.3531	0.0065	0.3274	0.0067
125	0.8842	0.0058	0.6353	0.0052	0.3757	0.0069	0.3518	0.0071
145	0.9318	0.0060	0.6681	0.0054	0.3946	0.0072	0.3711	0.0075
165	0.9609	0.0062	0.6943	0.0056	0.4142	0.0075	0.3884	0.0078
185	0.9992	0.0064	0.7154	0.0058	0.4220	0.0077	0.3955	0.0080
205	1.0027	0.0064	0.7320	0.0059	0.4250	0.0078	0.3978	0.0081
225	1.0137	0.0065	0.7306	0.0060	0.4254	0.0079	0.4009	0.0082
245	0.9997	0.0065	0.7248	0.0060	0.4202	0.0078	0.3933	0.0082
265	0.9709	0.0064	0.7134	0.0059	0.4103	0.0078	0.3805	0.0080
285	0.9461	0.0063	0.6923	0.0059	0.3953	0.0076	0.3578	0.0077
305	0.9222	0.0062	0.6703	0.0058	0.3742	0.0074	0.3272	0.0073
325	0.8807	0.0061	0.6396	0.0056	0.3519	0.0071	0.2844	0.0067
345	0.8145	0.0058	0.5941	0.0054	0.3312	0.0069	0.2546	0.0062
365	0.7615	0.0056	0.5580	0.0052	0.3006	0.0065	0.2316	0.0059
385	0.7226	0.0054	0.5216	0.0050	0.2788	0.0062	0.2105	0.0056
405	0.6475	0.0051	0.4781	0.0047	0.2576	0.0059	0.1923	0.0053
425	0.5987	0.0049	0.4390	0.0045	0.2279	0.0055	0.1740	0.0051
445	0.5432	0.0047	0.3920	0.0042	0.2068	0.0052	0.1553	0.0048
465	0.4744	0.0043	0.3499	0.0039	0.1802	0.0048	0.1378	0.0045
485	0.4178	0.0041	0.3009	0.0036	0.1592	0.0045	0.1187	0.0042
505	0.3639	0.0038	0.2667	0.0034	0.1378	0.0042	0.1062	0.0039
525	0.3269	0.0036	0.2321	0.0032	0.1190	0.0039	0.0910	0.0037

The benchmark values for the effective delayed neutron parameters are: $\beta_{\text{eff}} = 750 \pm 5$ pcm, $\Lambda = 31.96 \pm 1.06$ μ s, and $\beta_{\text{eff}}/\Lambda = 234.66 \pm 7.92$ s^{-1} .

All uncertainties given so far here are 1σ .

Although the intention of the reactor physics experiments performed by IPEN was not to evaluate critical configurations, an estimate of the total uncertainty and bias can be assigned to the k_{eff} of such critical experiments taking as reference the uncertainty evaluation of LEU.COMP.THERM.077 (Dos Santos et al., 2012d). In that evaluation the total uncertainty for the benchmark value of k_{eff} was 100 pcm and a bias of -33.5 pcm (due to the omission of the thermocouples and the detector and detector tubes in the benchmark model) was assigned. Due to the similarity of the core characteristics (same fuel rod, same core configuration, same moderator condition, etc.), this uncertainty and bias can both be assigned to the experimental k_{eff} of the critical configurations discussed here. Furthermore, it has been proven in the evaluation of the isothermal experiment that the total uncertainty and bias are not sensitive to the temperature. Moreover, in the same evaluation, it has been shown that the uncertainty of k_{eff} due to the control bank positioning and to the material and geometric data was negligible compared to the several other uncertainties. Therefore, the benchmark model for the critical configurations of the reactor physics experiments considered in this work is 1.00034 ± 0.00100 . This k_{eff} benchmark model will be referred to as assigned value because it was not included in the IRPhE handbook. This assigned k_{eff} benchmark value will be very helpful to interpret and to analyze the several calculated results of this work.

These benchmark values will serve as the reference values for the validation of the computer codes and associated nuclear data libraries considered in this work.

4. The calculation model results

This section shows the results of the deterministic and probabilistic calculations employing the HUEMUL-PUMA code system and MCNP5, respectively. The deterministic results based on the HUEMUL-PUMA code system will be shown in Section 4.1 while those of MCNP5 will be shown in Section 4.2.

Before discussing the calculation model results some explanation will be given to the nuclear data libraries used in the computer codes employed in this work. All criticality calculations performed by IPEN employed the ENDF/B-VI.8 nuclear data library (ENDF/B-VI, 2000). IPEN generated nuclear data libraries for MCNP5 at 20 °C and 80 °C from ENDF/B-VII.0 (Oblozinsky and Herman, 2006) and provided them to CNEA. CNEA by its turn made calculations with MCNP5 for all cases with these libraries and for some selected cases with ENDF/B-VI.8 of its own. For the temperature reactivity coefficient with MCNP5, IPEN employed the ENDF/B-VI.8 library. For the axial fission density distribution IPEN used MCNP5 with ENDF-VII.0 library and CNEA used both libraries, ENDF/B-VI.8 and ENF/B-VII.0. For the effective kinetic parameter calculations with MCNP5, IPEN provided results based on ENDF/B-VI.8 library, while CNEA based its calculations on the ENDF/B-VI.8 and ENDF/B-VII.0 and only the later one for the determination of the prompt neutron generation time (λ).

The deterministic HUEMUL code uses the WLUP-69 (<http://www-nds.iaea.org/wimsd/downloads.html>) library in the WIMS (Askew et al., 1966) format. The delayed neutron parameters used in this code system arises from the ENDF/B-VI.8 library.

4.1. The deterministic model results

4.1.1. Critical configurations

This sub-section shows the results of the deterministic calculations employing the HUEMUL-PUMA code system. Calculations regarding critical configurations presented in Section 3.1.1 will be presented in Section 4.2.1, together with the results coming from the probabilistic calculations, and it is understood that no special sub-section is needed here to show them. All the results presented in the PUMA analysis were based in a 5 group neutron structure.

4.1.2. The isothermal temperature coefficients

The general conditions of this experiment were shown in Section 3.1.2. The benchmark model, i.e., the reactor configuration and the schematic control bank positions are shown in Figs. 1 and 3, respectively. More details can be seen in reference Dos Santos et al. (2012a).

A cusping effect correction was used for a better reactivity and flux distribution calculations, and for different rod insertions. This effect arises when the rod insertion does not coincide with an exact number of axial pieces. For this case, when introducing partially the corresponding part of the control rod, its effect is diluted and this fact results in an overestimation of the control rod weight. In this case, the insertion position of the control rod is adjusted assuming a linear variation of the reactivity value of the control rod within de corresponding piece.

Table 2 shows the results, in units of percent withdrawn, of the critical control bank position employing the HUEMUL-PUMA code system. The control bank BC2 is always fixed at 60% withdrawal position and the control bank BC1 is adjusted to make the reactor critical according to the temperature. In HUEMUL-PUMA, the critical positions of the control bank BC1 are obtained maintaining the reactivity value at (110 ± 10) pcm.

Fig. 5 shows the comparison of the data of Table 2 against the measured values obtained by IPEN, extracted from Sections 1 and 3 of the reference report Dos Santos et al. (2012a). According to this comparison, HUEMUL-PUMA performs quite well when their results are compared to the measured values; thus indicating that the temperature effects on reactivity of the reactor system are calculated with a good level of accuracy.

In HUEMUL-PUMA critical rod positions of bank 1 are obtained maintaining the reactivity value in the range of (110 ± 10) pcm.

Table 2

Critical control bank positions (in units of percent withdrawn) as a function of temperature arising from the coupled HUEMUL-PUMA system calculations.

Temperature (°C)	BC1Withdrawal position (%)	BC2Withdrawal position (%)
20	56.4	60.0
30	57.4	60.0
40	58.9	60.0
50	60.7	60.0
60	63.4	60.0
70	66.7	60.0
80	70.4	60.0

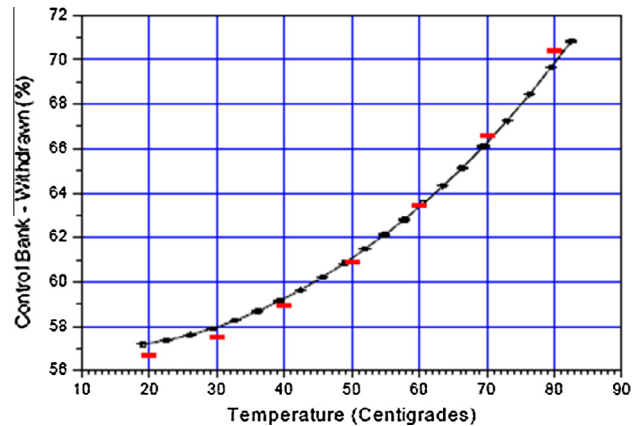


Fig. 5. Critical position of the control bank BC1 expressed in units of percent withdrawn, as a function of temperature given in °C. Red points correspond to values employing the coupled HUEMUL-PUMA systems and maintaining a reactivity value of (110 ± 10) pcm. (For interpretation of the references to color in this figure legend, the reader is referred to the web version of this article.)

Table 3

k_{eff} Values for 20 °C and 80 °C, for the control bank BC1 in the critical position.

Estimator	20 °C	80 °C	DELTA	α_{iso} error (pcm/°C)	Benchmark value (pcm/°C)
HUEMUL/PUMA	1.00160	1.00078	0.00082	-1.37	0.0 ± 0.1

Table 3 shows the comparison of the k_{eff} at BC1 critical control bank withdrawn position for 20 °C and 80 °C calculated by the HUEMUL-PUMA codes. The fourth column shows the k_{eff} difference (DELTA) between these two values in order to estimate the accuracy of the calculations. Table 3 shows that the HUEMUL-PUMA results are overestimated and a little bit outside of the range of the desired accuracy (± 1.0 pcm/°C (Santamarina, 1987)) for the determination of the reactivity coefficient even considering 3σ of the benchmark value. However, the HUEMUL-PUMA performance is much better than older evaluations, which historically show a discrepancy of approximately -4.0 pcm/°C (Edenius, 1976) and (Askew, 1973). Moreover, taken into consideration that the HUEMUL-PUMA code system is based on the multigroup diffusion theory with a main purpose for reactor design and analysis, this performance can be considered accurate enough.

4.1.3. Axial distribution of the fission density

The general conditions of all cases shown in this section have been described in Section 3.1.3. Reactor configuration in the x-y plane and the axial control bank positions are shown in Figs. 1 and 4, respectively. More details can be found in reference Dos Santos et al. (2012a). The calculated k_{eff} for this critical configuration

using HUEMUL-PUMA is 1.00261. This calculated k_{eff} is within 3σ of the assigned benchmark k_{eff} value (1.00034 ± 0.00100).

Figs. 6–12 show the comparison of calculated and measured values. These values were normalized consistently using de mean value of all fuel rods for which the measurements were available. There was no special normalization for any fuel rod. Figs. 6–12 compare calculated results obtained by HUEMUL-PUMA (crosses) with those from the benchmark-value results obtained by IPEN (continuous lines). The abscissa shows the axial positions in the active length of the fuel rod, and the ordinates show the relative fission densities. The theory–experiment comparisons attain to fuel rods that are close to the center of the core, close to the interface fuel-reflector, and close to the control banks. This fuel rod selection covers a wide range of possibilities and makes the analyses complete and helpful.

All experimental results are from reference Dos Santos et al. (2012a), Section 3.

The agreement between HUEMUL-PUMA and the benchmark-values are pretty good, thus showing the ability of this code system to predict fission density shapes in a variety of situations. The mean square error was 5.5% and the highest deviation between calculated and benchmark values were 15% which occurred in the interface core-reflector; region where diffusion theory shows deficiencies.

4.1.4. Effective delayed neutron parameters

The general conditions for this experiment have been defined in reference Dos Santos et al. (2012a) and some details were given in Section 3.1.4. Reactor configuration and the x–y plane and axial control bank positions are shown in Figs. 1 and 4, respectively. More details can also be seen in reference Dos Santos et al. (2012a).

The effective kinetics parameters to be calculated are defined according to point kinetics theory (Bell and Glasstone, 1979) as:

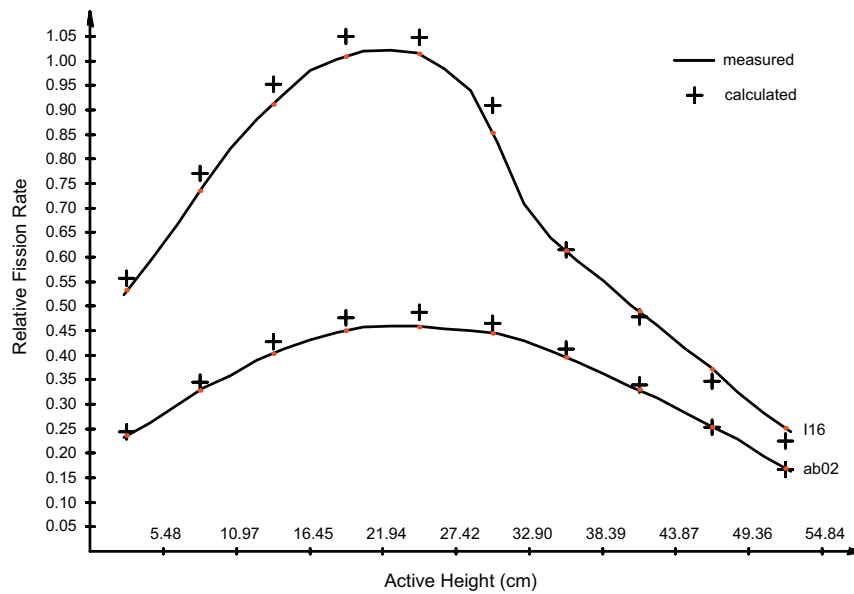


Fig. 6. Calculated and measured normalized fission density distribution for fuel rods I16 and ab02.

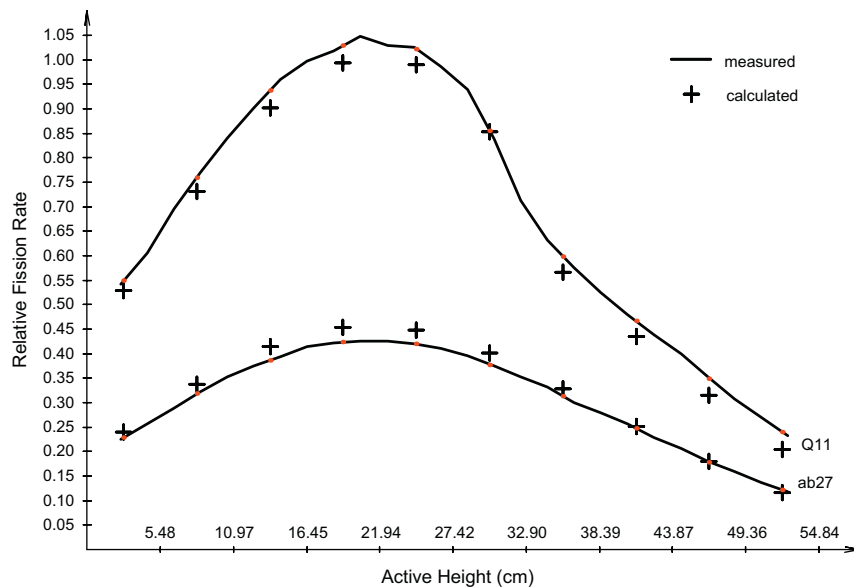


Fig. 7. Calculated and measured normalized fission rate distribution for fuel rods Q11 and ab27.

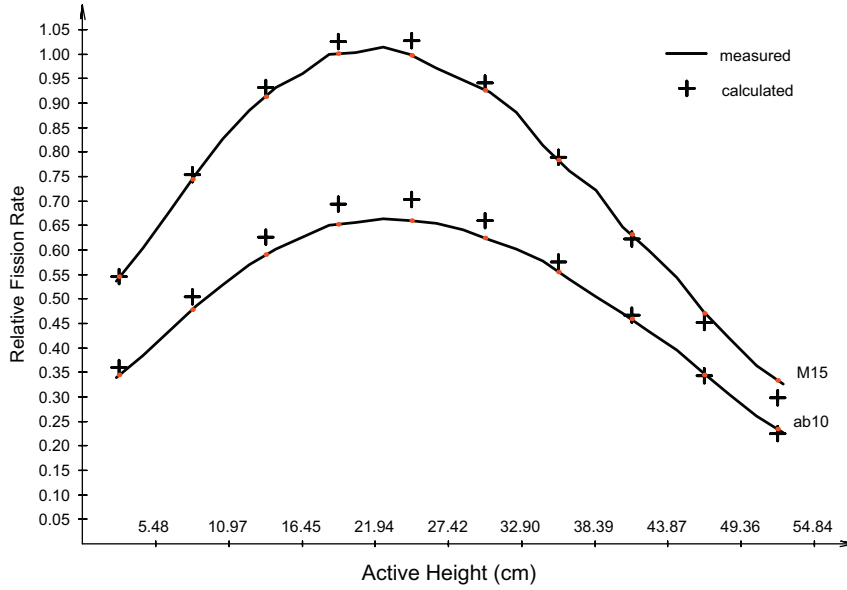


Fig. 8. Calculated and measured normalized fission density distribution for fuel rods M15 and ab10.

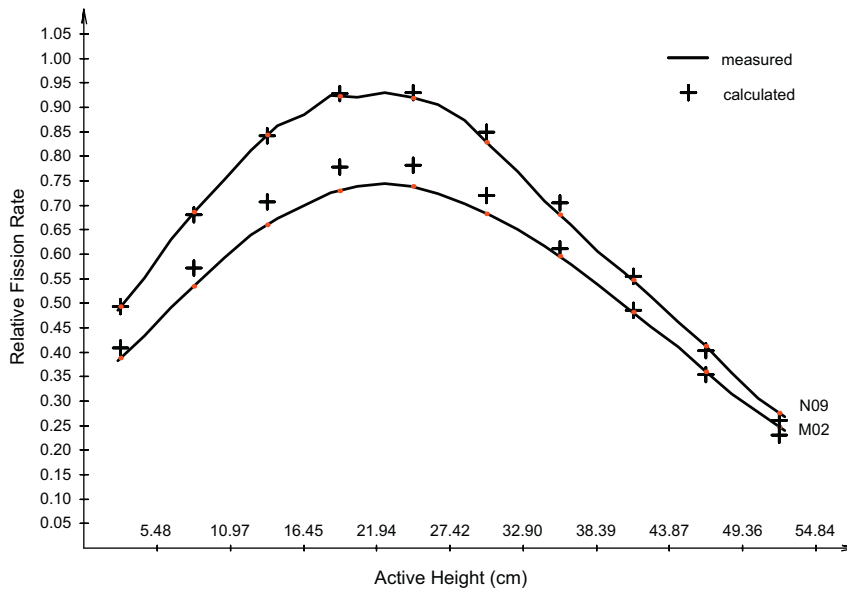


Fig. 9. Calculated and measured normalized fission density distribution for fuel rods N09 and M02.

$$\beta_{effj} = \frac{1}{F} \int_V \left(\sum_g \chi_{jg} \phi_g^* \right) \beta_j \left(\sum_g \nu \Sigma_{fg} \phi_g \right) dr^3 \quad (3)$$

$$\beta_{eff} = \sum_j \beta_{effj} \quad (4)$$

$$A = \frac{n}{F} \quad (5)$$

where:

$$n = \int_V \sum_g \phi_g^* \frac{\Phi_g}{\nu_g} dr^3 \quad (6)$$

$$F = \int_V \left(\sum_g \chi_{g} \phi_g^* \right) \left(\sum_g \nu \Sigma_{fg} \phi_g \right) dr^3 \quad (7)$$

The subscripts g and j represent respectively the neutron energy group and the family of the delayed neutron precursor, the superscript (*) represents the adjoint function, β_j represents the delayed neutron fraction of family j , β_{effj} represents the effective delayed neutron fraction of family j , β_{eff} is the effective delayed neutron fraction, V represents the volume, χ_{jg} , and χ_g represent respectively the fission neutron spectra of the delayed and prompt neutrons, ϕ_g represents the neutron flux, and $\nu \Sigma_{fg} \phi_g$ is the total neutron production by fissions per unit volume and time.

The critical control bank positions for the calculation of the effective kinetic parameters are equal to 58.9% withdrawn position and for this condition the 5 group direct and adjoint fluxes distributions were evaluated employing HUEMUL-PUMA. The calculated k_{eff} for this critical configuration using HUEMUL-PUMA is 1.00261 which is again within 3σ of the assigned benchmark k_{eff} value (1.00034 ± 0.00100). Next, the HUEMUL-PUMA code system solves the direct and adjoint diffusion equations to get the adjoint and

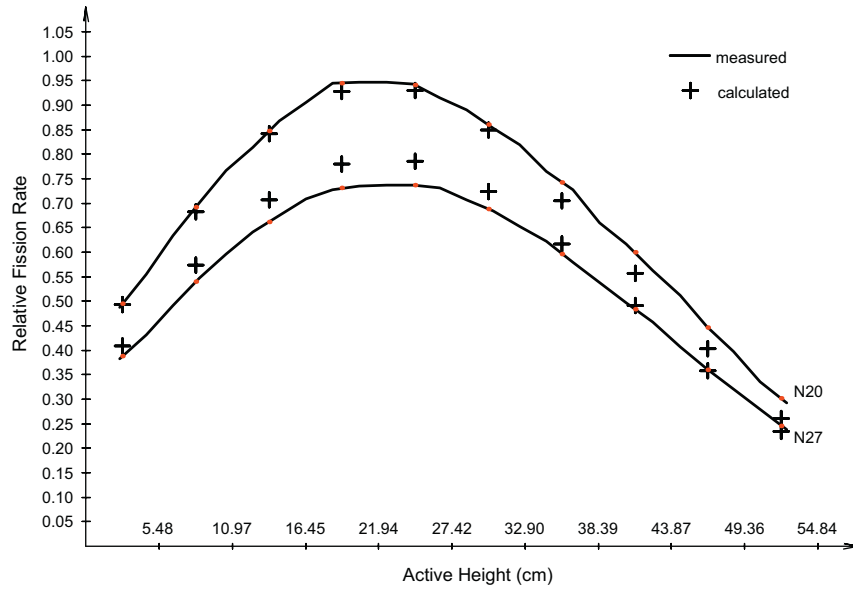


Fig. 10. Calculated and measured normalized fission density distribution for fuel rods N20 and N27.

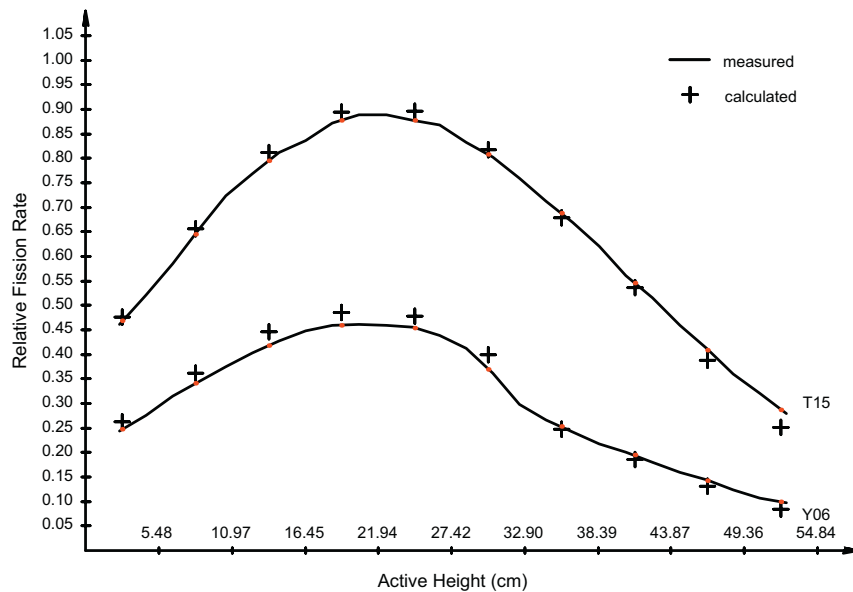


Fig. 11. Calculated and measured normalized fission density distribution for fuel rods T15 and Y06.

direct fluxes. These fluxes were inserted into Eqs. (3)–(7) to get the effective delayed neutron parameters. Table 4 shows the results of HUEMUL-PUMA together with the benchmark values provided by IPEN. The agreement can be considered very satisfactory for these sort of nuclear data parameters. All calculated results are within 3σ of the benchmark values.

4.2. Probabilistic models: MCNP5

MCNP5 was employed in all the benchmark analyses of this work. Since this code is very flexible and capable of modeling explicitly all the core configurations of the IPEN/MB-01 reactor, it was used extensively to verify the quality of the nuclear data libraries ENDF/B-VI.8 and ENDF/B-VII.0.

4.2.1. Criticality calculations

MCNP5 runs were performed for some selected cases in order to evaluate k_{eff} results, with 100000 neutrons per cycle and 6500 cycles, obtained from the ENDF/B.VI.8 library, and some other cases with nuclear data from the ENDF/B.VII.0 library. Table 5 shows the MCNP5-CNEA, MCNP5-IPEN and the HUEMUL-PUMA k_{eff} results. Table 5 also shows the benchmark values from references Dos Santos et al. (2012a–2012j); the MCNP5 results must be compared to these values. In general terms, the ENDF/B-VII.0 results show a tendency to overestimate k_{eff} . Good part of this overestimation (Van der Marck, 2006) may be credited to the scattering law of Hydrogen bound in water which was generated from the $S(\alpha, \beta)$ function of ENDF/B-VII.0. The ENDF/B-VI.8 k_{eff} results are mostly underestimated which are a well known behavior from several other benchmark analyses performed (Van der

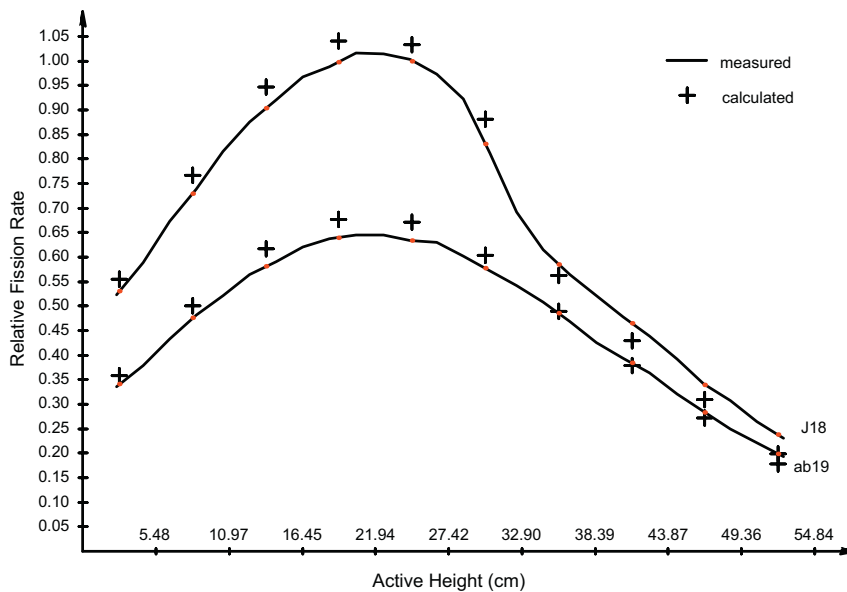


Fig. 12. Calculated and measured normalized fission density distribution for fuel rods J18 and ab19.

Table 4

Comparison of results obtained by means of HUEMUL and PUMA codes and those obtained by IPEN.

Effective kinetic parameter	CNEA HUEMUL-PUMA	Benchmark value	$(C - E) / E * 100$
β Nuclear (pcm)	688	–	–
β_{eff} (pcm)	741.00	750 ± 5	–1.2
Λ (μ s)	30.72	31.96 ± 1.06	–3.88
$\beta_{eff} \Lambda$ (s^{-1})	241.12	234.66 ± 7.92	2.75

Marck and Hogenbirk, 2003) with this library. The HUEMUL-PUMA k_{eff} results are all within 3σ of the range of the benchmark value which make the performance of this code system quite good. Consequently this code system is capable to predict k_{eff} in critical situations with an accuracy of at least 300 pcm in the worst case.

4.2.2. Fission density axial distribution

Tables 6 and 7 show the theory–experiment comparison of the fission densities obtained by IPEN and CNEA for some selected fuel rod positions. IPEN employed MCNP5 with ENDF/B-VII.0 library while CNEA uses the same code but with ENDF/B-VI.8 and ENDF/B-VII.0 nuclear data libraries; each run was performed for 650 cycles with 3×10^6 neutrons per cycle. Both tables show the relative experimental uncertainty (in units of %) and the quantity $(C - E) / E$,

where C and E are, respectively, the calculated and the experimental relative fission densities. With exception of the positions close to the core-reflector interface, an excellent agreement was found with most of the calculated axial points within 3σ of the experimental value.

4.2.3. Isothermal temperature experiment

Table 8 shows the MCNP5 k_{eff} results at 20 °C and 80 °C from IPEN and CNEA. The k_{eff} results of CNEA were obtained with ENDF/B-VII.0 while those of IPEN were obtained with ENDF/B-VI.8; each run was performed for 4500 cycles with 2×10^6 neutrons per cycle. As already mentioned previously the ENDF/B-VII.0 results are a little bit overestimated due mainly due to the $S(\alpha, \beta)$ scattering law of Hydrogen bound in the water which was originated from ENDF/B-VII.0. The ENDF/B-VI.8 k_{eff} results are all underestimated, which are in perfect agreement to several other benchmark analyses using this library (Van der Marck and Hogenbirk, 2003).

Table 9 shows the k_{eff} difference (DELTA) between 20 °C and 80 °C and the corresponding average α_{iso} error between these two temperatures from both institutions: IPEN and CNEA. Table 9 shows that both ENDF/B-VI.8 and ENDF/B-VII.0 overestimates the isothermal reactivity coefficient independently of the k_{eff} estimator considered. However, the general performance is much better than older evaluations, which historically show a discrepancy of

Table 5

k_{eff} Results from MCNP-IPEN, MCNP-CNEA, and from deterministic code HUEMUL-PUMA for some selected cases.

References	CASE	MCNP-IPEN [ENDF/B-VI.8]	MCNP-CNEA [ENDF/B-VI.8]	MCNP-CNEA [ENDF/B-VII.0]	HUEMUL-PUMA	Benchmark Value
Dos Santos et al. (2012b)	1	0.9993 ± 0.0001	^a	1.0020 ± 0.0002	1.0024	1.0007 ± 0.0010
	2	0.9997 ± 0.0001	^a	1.0016 ± 0.0002	1.0029	1.0008 ± 0.0010
	3	0.9994 ± 0.0001	0.9997 ± 0.0002	1.0021 ± 0.0002	1.0022	1.0006 ± 0.0010
Diniz and Dos Santos (2006)	9	0.9984 ± 0.0001	^a	1.0017 ± 0.0003	1.0001	1.0004 ± 0.0010
Diniz and Dos Santos (2002)	6	0.9978 ± 0.0001	0.9969 ± 0.0003	1.0008 ± 0.0003	0.9978	1.0005 ± 0.0010
Dos Santos et al. (2012a)	5	1.0007 ± 0.0001	^a	1.0056 ± 0.0003	0.9995	1.0003 ± 0.0010
Dos Santos et al. (2012c)	1	0.9991 ± 0.0001	0.9992 ± 0.0002	1.0032 ± 0.0002	1.0034	1.0007 ± 0.0010
Dos Santos et al. (2012d)	1	0.9978 ± 0.0001	0.9978 ± 0.0002	1.0016 ± 0.0002	1.0012	1.0004 ± 0.0010
Dos Santos et al. (2012e)	4	0.9968 ± 0.0001	0.9980 ± 0.0002	1.0018 ± 0.0001	0.9997	1.0003 ± 0.0010
Dos Santos et al. (2012f)	6	0.9983 ± 0.0001	^a	1.0008 ± 0.0003	1.0029	1.0005 ± 0.0010
Dos Santos et al. (2012g)	6	0.9981 ± 0.0001	^a	^a	1.0001	1.0006 ± 0.0010

^a Not evaluated.

Table 6
MCNP5 relative fission density comparisons.

Axial cote (mm)	POSITION M15				POSITION M27			
	EXP.	(C – E)/E (%)	(C – E)/E (%) ENDF/	(C – E)/E (%) ENDF/	EXP.	(C – E)/E (%)	(C – E)/E (%) ENDF/	(C – E)/E (%) ENDF/
	UNCERT (%)	ENDF/B-VII.0 IPEN	B-VII.0 CNEA	B-VI.8 CNEA	UNCERT (%)	ENDF/B-VII.0 IPEN	B-VII.0 CNEA	B-VI.8 CNEA
25	0.76	6.82	17.30	18.06	0.76	3.52	15.75	17.09
45	0.75	6.22	-0.78	-0.68	0.75	1.74	1.01	1.78
65	0.71	4.42	0.83	0.84	0.71	2.46	0.84	0.47
85	0.69	3.50	1.44	1.23	0.69	0.76	1.61	1.33
105	0.67	3.27	1.50	0.96	0.67	0.11	2.57	2.37
125	0.66	2.66	2.08	1.76	0.90	0.65	2.60	1.56
145	0.64	2.47	2.51	2.59	0.87	-0.13	2.80	1.30
165	0.65	1.15	3.26	3.04	0.84	-0.47	2.66	1.74
185	0.64	2.52	2.45	2.05	0.83	-0.19	2.75	1.87
205	0.64	1.09	4.06	3.25	0.82	0.18	2.19	0.70
225	0.64	1.66	3.08	1.92	0.82	-0.31	2.12	0.71
245	0.65	1.09	2.97	2.23	0.81	-0.09	1.16	0.95
265	0.66	-0.07	3.49	3.08	0.81	0.64	-0.18	0.77
285	0.67	0.61	2.43	2.17	0.81	0.31	-0.74	0.33
305	0.67	2.56	0.20	-0.26	0.81	1.40	-1.60	-1.69
325	0.69	3.30	-0.10	-1.04	0.82	2.06	-1.86	-3.21
345	0.71	2.68	1.87	1.15	0.83	0.62	-0.37	-1.53
365	0.74	2.82	1.39	1.01	0.83	1.83	-1.34	-1.09
385	0.75	4.31	-0.84	-1.76	0.85	2.72	-2.38	-1.25
405	0.79	1.63	1.50	0.59	0.87	3.35	-2.57	-1.40
425	0.82	4.37	-0.90	-0.72	0.88	4.24	-3.58	-3.19
445	0.87	5.54	-1.62	-1.77	0.91	4.09	-2.37	-2.12
465	0.91	4.28	0.34	-1.31	0.93	4.62	-3.14	-3.34
485	0.98	5.69	-1.34	-2.80	0.96	3.84	-1.89	-3.39
505	1.04	7.75	-3.60	-3.60	0.98	7.41	-4.69	-6.49
525	1.10	11.11	5.60	5.66	1.03	8.96	4.35	3.83

Table 7
MCNP5 relative fission density comparisons.

Axial cote (mm)	POSITION ab27				POSITION B24			
	EXP.	(C – E)/E (%)	(C – E)/E (%) ENDF/	(C – E)/E (%) ENDF/	EXP.	(C – E)/E (%)	(C – E)/E (%) ENDF/	(C – E)/E (%) ENDF/
	UNCERT. (%)	ENDF/B-VII.0 IPEN	B-VII.0 CNEA	B-VI.8 CNEA	UNCERT. (%)	ENDF/B-VII.0 IPEN	B-VII.0 CNEA	B-VI.8 CNEA
25	2.00	3.87	13.45	14.65	2.21	6.41	16.82	16.16
45	1.94	3.13	-1.56	-0.35	2.18	5.71	-1.72	-1.01
65	1.90	1.61	-0.42	0.45	2.12	4.36	-1.19	-0.89
85	1.86	2.04	-1.42	-0.40	2.07	3.84	-0.03	-0.67
105	1.84	2.63	-2.38	-0.71	2.05	3.78	0.86	-0.34
125	1.84	1.68	-1.49	-0.35	2.02	4.34	-0.14	-0.54
145	1.82	0.91	-0.35	-0.15	2.02	2.99	-0.51	-0.86
165	1.81	2.18	-0.68	-1.30	2.01	4.48	-0.70	-1.75
185	1.82	1.23	-0.95	-1.78	2.02	3.25	-0.78	-0.40
205	1.84	0.75	-2.07	-2.24	2.04	3.04	-1.41	0.96
225	1.86	0.86	-2.70	-1.67	2.05	4.20	-2.87	-0.80
245	1.86	1.42	-2.26	-2.02	2.08	3.95	-2.39	-1.70
265	1.90	1.49	-2.46	-3.61	2.10	3.74	-3.31	-2.94
285	1.92	2.42	-4.20	-4.15	2.15	3.48	-4.81	-6.34
305	1.98	2.06	-4.49	-3.98	2.23	4.25	-6.57	-9.47
325	2.02	1.86	-4.12	-4.58	2.36	5.89	-5.91	-6.68
345	2.08	3.33	-5.65	-5.89	2.44	7.54	-6.79	-5.30
365	2.16	1.42	-4.16	-4.03	2.55	7.57	-6.95	-5.57
385	2.22	3.72	-5.34	-6.28	2.66	7.91	-6.03	-5.27
405	2.29	5.53	-7.88	-7.61	2.76	8.85	-5.77	-5.25
425	2.41	3.76	-6.01	-3.95	2.93	9.59	-6.55	-6.72
445	2.51	6.11	-6.48	-5.71	3.09	10.51	-6.83	-7.28
465	2.66	4.81	-4.66	-5.49	3.27	12.25	-7.26	-7.55
485	2.83	7.08	-6.85	-8.29	3.54	11.37	-8.93	-7.25
505	2.00	8.75	-8.06	-10.52	3.67	16.03	-14.69	-12.71
525	1.94	9.56	1.93	-1.60	4.07	16.47	-1.10	-0.33

approximately -4.0 pcm/ $^{\circ}$ C Edenius (1976) and Askew (1973). In general terms, these characteristics may be credited to the new ^{235}U η -shape (Weigmann et al., 1990), which was incorporated in the evaluation of the nuclear data library used in this work. These improved cross sections made the theory–experiment comparisons come into a better agreement. ENDF/B-VI.8 and ENDF/B-VII.0 show a performance that, even considering the errors due to the Monte Carlo approach (1σ), meet the desired accuracy

(± 1.0 pcm/ $^{\circ}$ C (Santamarina, 1987)) for the isothermal reactivity coefficient determination. The performance of the calculations of both institutions is excellent and attends the desired accuracy for the determination of the reactivity coefficient.

4.2.4. Effective kinetic parameters

Two separated MCNP5 k_{eff} calculations were required to obtain β_{eff} (Bretscher, 1997): one to obtain k_1 (multiplication factor with-

Table 8
MCNP5 k_{eff} values at 20 °C and 80 °C from IPEN and CNEA.

Estimator	IPEN [ENDF/B.VI.8] 20 °C	CNEA [ENDF/B.VII.0] 20 °C	IPEN [ENDF/B.VI.8] 80 °C	CNEA [ENDF/B.VII.0] 80 °C	Assigned benchmark k_{eff} value
Collision	0.99791 ± 0.00007	1.00162 ± 0.00005	0.99757 ± 0.00007	1.00120 ± 0.00006	1.00034 ± 0.00100
Absorption	0.99786 ± 0.00005	1.00162 ± 0.00004	0.99760 ± 0.00005	1.00118 ± 0.00005	1.00034 ± 0.00100
Track length	0.99788 ± 0.00008	1.00162 ± 0.00007	0.99749 ± 0.00008	1.00118 ± 0.00007	1.00034 ± 0.00100
Col/Absorp	0.99789 ± 0.00005	1.00162 ± 0.00004	0.99759 ± 0.00005	1.00119 ± 0.00005	1.00034 ± 0.00100
Abs/trk len	0.99787 ± 0.00005	1.00162 ± 0.00004	0.99757 ± 0.00005	1.00118 ± 0.00005	1.00034 ± 0.00100
Col/trk len	0.99790 ± 0.00006	1.00162 ± 0.00005	0.99755 ± 0.00006	1.00119 ± 0.00005	1.00034 ± 0.00100
Col/abs/trk len	0.99786 ± 0.00005	1.00162 ± 0.00004	0.99757 ± 0.00005	1.00118 ± 0.00004	1.00034 ± 0.00100

Table 9
MCNP5 DELTA k_{eff} and α_{iso} error values from IPEN and CNEA.

Estimator	IPEN		CNEA	
	DELTA	α_{iso} error (pcm/°C)	DELTA	α_{iso} error (pcm/°C)
Collision	0.00034	-0.57 ± 0.17	0.00042	-0.70 ± 0.13
Absorption	0.00026	-0.44 ± 0.12	0.00044	-0.73 ± 0.11
Track length	0.00039	-0.65 ± 0.19	0.00044	-0.73 ± 0.16
Col/Absorp	0.00030	-0.50 ± 0.12	0.00043	-0.71 ± 0.11
Abs/trk len	0.00030	-0.50 ± 0.12	0.00044	-0.73 ± 0.11
Col/trk len	0.00035	-0.59 ± 0.14	0.00043	-0.71 ± 0.12
Col/abs/trk len	0.00029	-0.49 ± 0.12	0.00044	-0.73 ± 0.09

out delayed neutron contribution) and the other one for k_0 (multiplication factor with prompt and delayed neutron contributions). Afterwards, β_{eff} is calculated with k_0 and k_1 making use of Eq. (8):

$$B_{eff} = 1 - k_1/k_0 \quad (8)$$

The prompt neutron generation time (Λ) was obtained by means of the insertion method $1/\nu$ (Bretschler, 1997) where ν is the neutron velocity. This is achieved using first order perturbation theory through the dilution, uniformly distributed, of a pure neutron absorber of $1/\nu$ type. The fractional change of the eigenvalue (the multiplication factor) is given by:

$$\begin{aligned} \frac{\delta k}{k_p} &= k_0 \int_E dE \int_{\Omega} d\Omega \int_V dV dr^3 [\varphi^*(\vec{r}, E, \hat{\Omega}) \varphi(\vec{r}, E, \hat{\Omega}) \delta \sum_a(\vec{r}, E)] / F \\ \frac{\delta k}{k_p} &= N \sigma_{ao} \nu_0 k_0 \int_E dE \int_{4\pi} d\Omega \int_V dV dr^3 [\varphi^*(\vec{r}, E, \hat{\Omega}) \varphi(\vec{r}, E, \hat{\Omega}) \delta \sum_a(\vec{r}, E)] / F \\ \frac{\delta k}{k_p} &= N \sigma_{ao} \nu_0 k_0 \Lambda'_p \end{aligned} \quad (9)$$

where N is the concentration (atoms/b-cm) of $1/\nu$ absorber whose absorption cross section is σ_{ao} for neutrons with speed ν_0 ; k_p and k_0 are the eigenvalues of perturbed and unperturbed cases respectively; Λ'_p is the prompt neutron generation time for the perturbed case.

The prompt neutron generation time is obtained from Eq. (10) when N tends to zero:

$$\Lambda = \lim_{N \rightarrow 0} \Lambda'_p = \lim_{N \rightarrow 0} (\delta k/k_p) / (N \sigma_{ao} \nu_0 k_0) \quad (10)$$

Two separate calculations were performed with MCNP to determine the Λ value. Parameters k_0 and k_p are the effective multiplication factors from such MCNP runs considering very diluted absorber concentrations (in the range of 10^{-9} to 10^{-8} atoms/b-cm). The prompt neutron generation time was obtained extrapolating linearly the Λ'_p values which depend of the absorber concentration N for the value corresponding to $N = 0$.

Table 10 shows the comparison of the results from the MCNP calculations by the CNEA, using ENDF/B.VI.8 and ENDF/B.VII.0 (each run was performed for 4500 cycles with 2×10^6 neutrons per cycle) to those obtained by IPEN using the library ENDF/

Table 10
Effective kinetic parameters.

Kinetic parameter	MCNP5-IPEN [ENDF/B-VI.8]	MCNP5-CNEA [ENDF/B-VI.8]	MCNP5-CNEA [ENDF/B-VII.0]	Benchmark value
β_{eff} (pcm)	791.6 ± 4.1	785 ± 13	754 ± 10	750 ± 5
Λ (μ s)	29.65 ^a	^b	34.8 ± 8.2	31.96 ± 1.06

^a Calculated by TORT using library ENDF/B-VI.8.

^b Due to the high computer time needed to obtain Λ , this parameter was calculated only with ENDF/B.VII.0.

B.VI.8. The agreement of the ENDF/B-VII.0 β_{eff} result to the benchmark value is excellent, which is in perfect agreement to other work (Van der Marck, 2006). In contrast, ENDF/B-VI.8 overestimates β_{eff} . The prompt neutron generation time (Λ) is underestimated by IPEN. On the other hand, the value obtained by CNEA is statistically equivalent to the benchmark value.

5. Conclusions

5.1. Deterministic calculations

The HUEMUL-PUMA computer code system predicts the k_{eff} benchmark values always within a range of ± 300 pcm; it has a tendency to overestimate k_{eff} values with respect to the results obtained with MCNP5 in most cases.

Considering the reactor physics experiments of reference Dos Santos et al. (2012a), HUEMUL-PUMA performs very well for the effective delayed neutron parameters. These data follow the standard way of the point kinetic model, weighting the integral expressions with the adjoint flux.

The critical control bank as a function of temperature was very well reproduced by HUEMUL-PUMA (see Fig. 5).

The spatial fission density distribution (Figs. 6–12) shows a very good agreement to the experimental values taking into account that diffusion theory calculation is used.

5.2. Stochastic calculations

Similarly to other works, the results of MCNP5 with ENDF/B-VI.8 underestimate the k_{eff} values relatively to the benchmark values. The deviation in some cases is even outside of the 3σ range of the benchmark values. On the other hand, when ENDF/B-VII.0 is used in conjunction with MCNP5, the agreement is improved and the differences between calculated and benchmark values are inside of the 3σ range of the benchmark values.

The analysis of the fission density experiments with MCNP5 reveals that, with exception to the points close to the reflector interface, both institutions perform well and most of the calculated points are within 3σ of the experimental values.

Regarding the isothermal temperature coefficient experiment, the ENDF/B-VII.0 k_{eff} results are a little bit overestimated due mainly due to the $S(\alpha, \beta)$ scattering law of Hydrogen bound in

the water which was originated from ENDF/B-VII.0. The ENDF/B-VI.8 k_{eff} results are all underestimated, which are in perfect agreement to several other benchmark analyses using this library (Van der Marck and Hogenbirk, 2003). For the isothermal temperature analysis, ENDF/B-VI.8 and ENDF/B-VII.0 show a performance that, even considering the errors due to the Monte Carlo approach (1σ), meet the desired accuracy (± 1.0 pcm/ $^{\circ}$ C (Santamarina, 1987)) for the isothermal reactivity coefficient determination. The performance of the calculations of both institutions is excellent and attends the desired accuracy for the determination of the reactivity coefficient.

The agreement of the ENDF/B-VII.0 β_{eff} result to the benchmark value is excellent, which is in perfect agreement to other work (Van der Marck, 2006). In contrast, ENDF/B-VI.8 overestimates β_{eff} . The prompt neutron generation time (Λ) is underestimated by IPEN. On the other hand, the value obtained by CNEA is statistically equivalent to the benchmark value.

Acknowledgements

Authors thank to the authorities of CNEA (Argentina) and CNEN (Brazil) which in the frame of COBEN (Nuclear Energy Argentine-Brazilian Agreement) have made it possible to carry out this project.

References

- Askew, J., 1973. Thermal Reactor Temperature Coefficients. AEEW-R-886, U.K. Atomic Energy Agency.
- Askew, J.R., Fayers, F.J., Kemshell, P.B., 1966. A general description of the lattice code WIMS. J. Brit. Nucl. Energy Soc. 5, 564.
- Bell & Glasstone, 1979. Nuclear Reactor Theory. Robert E. Krieger Publishing Company, New York.
- Bretscher, M.M., 1997. RERTR Program Argonne National Laboratory Argonne, IL 60439-4841, USA. Perturbation – Independent Methods for Calculating Research Reactor Kinetic Parameters.
- Briggs, J.B. (Ed.), 2012a. International Handbook of Evaluated Criticality Safety Benchmark Project. NEA/NSC/DOC (95)03. Nuclear Energy Agency, OECD, Paris, France.
- Briggs, J.B. (Ed.), 2012b. International Handbook of Evaluated Reactor Physics Benchmark Experiments. Nuclear Energy Agency (NEA DATA BANK, Paris, France).
- Diniz, R., Dos Santos, A., 2002. A noise analysis approach for measuring the decay constants and the relative abundance of delayed neutrons in a zero power critical facility. J. Nucl. Sci. Technol. (Supplement 2), 669–672.
- Diniz, R., Dos Santos, A., 2006. Experimental determination of the decay constants and abundances of delayed neutrons by means of reactor noise analysis. Nucl. Sci. Eng. 152, 125–141.
- Dos Santos, A., Pasqualeto, H., Fanaro, L.C.C.B., Fuga, R., Jerez, R., 1999. The inversion point of the isothermal reactivity coefficient of the IPEN/MB-01 Reactor – 1: Experimental procedure. Nucl. Sci. Eng. 113, 314.
- Dos Santos, A., et al., 2012a. IPEN (MB01)-LWR- CRIT-SPEC-REAC-COEF-KIN-RRATE-POWDIS-001: reactor physics experiments in the IPEN/MB-01 research reactor facility, International Handbook of Evaluated Reactor Physics Benchmark Experiments. Paris: Nuclear Energy Agency (NEA DATA BANK), pp. 1–142.
- Dos Santos, A., Fanaro, L.C.C.B., Yamaguchi, M., Jerez, R., Silva, G.S.A., Siqueira, P.T.D., Abe, A.Y., Fuga, R., 2012b. Critical loading configurations of the IPEN/MB-01 reactor with a heavy SS-304 reflector, LEU-COMP-THERM-043. In: Briggs, J. Blair (Ed.), International Handbook of Evaluated Criticality Safety Benchmark Experiments. NEA/NSC/DOC (95)03/l. Paris, September.
- Dos Santos, A., et al., 2012c. Critical loading configurations of the IPEN/MB-01 Reactor with UO₂, stainless steel and copper rods, LEU-COMP-THERM-044. In: Briggs, J. Blair (Ed.), International Handbook of Evaluated Criticality Safety Benchmark Experiments. NEA/NSC/DOC (95)03/l. Paris, September.
- Dos Santos, A., et al., 2012d. Critical loading configurations of the IPEN/MB-01 reactor, LEU-COMP-THERM-077. In: Briggs, J. Blair (Ed.), International Handbook of Evaluated Criticality Safety Benchmark Experiments. NEA/NSC/DOC (95)03/l. Paris, September.
- Dos Santos, A., et al., 2012e. Critical loading configurations of the IPEN/MB-01 reactor with low enriched fuel and burnable poison rods, LEU-COMP-THERM-082. In: Briggs, J. Blair (Ed.), International Handbook of Evaluated Criticality Safety Benchmark Experiments. NEA/NSC/DOC (95)03/l. Paris, September.
- Dos Santos, A., et al., 2012f. Critical loading configurations of the IPEN/MB-01 reactor with a big central void, LEU-COMP-THERM-083. In: Briggs, J. Blair (Ed.), International Handbook of Evaluated Criticality Safety Benchmark Experiments. NEA/NSC/DOC (95)03/l. Paris, September.
- Dos Santos, A., et al., 2012g. Critical loading configurations of the IPEN/MB-01 reactor with a central cruciform rod, LEU-COMP-THERM-084. In: Briggs, J. Blair (Ed.), International Handbook of Evaluated Criticality Safety Benchmark Experiments. NEA/NSC/DOC (95)03/l. Paris, September.
- Dos Santos, A., et al., 2012h. Critical loading configurations of the IPEN/MB-01 reactor with UO₂ and borated stainless steel plates, LEU-COMP-THERM-089. In: Briggs, J. Blair (Ed.), International Handbook of Evaluated Criticality Safety Benchmark Experiments. NEA/NSC/DOC (95)03/l. Paris, September.
- Dos Santos, A., et al., 2012i. Critical loading configurations of the IPEN/MB-01 reactor with UO₂ and stainless steel rods, LEU-COMP-THERM-090. In: Briggs, J. Blair (Ed.), International Handbook of Evaluated Criticality Safety Benchmark Experiments. NEA/NSC/DOC (95)03/l. Paris, September.
- Dos Santos, A., et al., 2012j. Critical loading configurations of the IPEN/MB-01 reactor with UO₂, stainless steel and Gd₂O₃ Rods, LEU-COMP-THERM-091. In: Briggs, J. Blair (Ed.), International Handbook of Evaluated Criticality Safety Benchmark Experiments. NEA/NSC/DOC (95)03/l. Paris, September.
- Edenius, M., 1976. Studies of the Reactivity Temperature Coefficient in Light Water Reactor. AE-RF-76-3160.
- ENDF/B-VI Summary Documentation, 2000. BNL-NCS-17451 (ENDF-201) (ENDF/B-VI). In: Rose, P.F. (Ed.), National Nuclear Data Center, Brookhaven National Laboratory, Release-8, fourth ed., 2000.
- Grant, C., 2011. Manual del Código PUMA Versión 6. Internal Report CNEA: MCO-06-REC-2.
- Grant, C., 2012. Manual del Código HUEMUL Versión 4. Internal Report CNEA: MCO-06-REC-1.
- Grant, C., et al., 2011. Validación de Sistemas y Modelos de Cálculo Neutrónico por medio de casos de referencia en el marco de la Comisión Binacional de Energía Nuclear. CNEA, ITE-06-REC-240.
- Kobayashi, I., Tsuruta, H., Hashimoto, M., Abe, S., Kodaira, T., Ogura, S., 1978. Critical Experiment and Analysis on the Core for Japan First Nuclear Ship Reactor. JAERI-1166, September.
- Kuramoto, R.Y.R. et al., 2006. Absolute measurement of β_{eff} based on feynman- α experiments and the two-region model in the IPEN/MB-01 research reactor. Annu. Nucl. Energy 34 (6), 433–442.
- Kuramoto, R.Y.R. et al., 2008. Absolute measurement of β_{eff} based on Rossi- α experiments and the two-region model in the IPEN/MB-01 research reactor. Nucl. Sci. Eng. 158, 272–283.
- Myioh, Y., Itagaki, M., Akai, M., 1993. A Geometric Buckling Expression for Regular Polygons: I. Measurements in Low-Enriched UO₂-H₂O Lattices. JAERI-3190-11, January.
- Oblozinsky, O., Herman, M., 2006. Special issue on evaluated nuclear data file ENDF/B-VII.0. Nucl. Data Sheets 107 (12).
- Reus, U., Westmeier, W., 1983. Atomic Data and Nuclear Data Tables. vol. 29, issue 1, July, pp. 1–192.
- Sakurai, T. et al., 1999. Measurement of effective delayed neutron fraction β_{eff} by ²⁵²Cf source method for benchmark: experiments of β_{eff} at FCA. Prog. Nucl. Energy 35 (2), 195–202.
- Santamarina, A., 1987. Nuclear Data for the Calculation of Thermal Reactor RTC. IAEA-TECDOC-491, Vienna, 7–10 December.
- Spriggs, G.D., 1993. Two-Rossi- α techniques for measuring the effective delayed neutron fraction. Nucl. Sci. Eng. 113, 161–172.
- Spriggs, G.D. et al., 1997. Two-region kinetic model for reflected reactors. Ann. Nucl. Energy 24 (3), 205.
- Van der Marck, S.C., 2006. Benchmarking ENDF/B-VII.0. Nucl. Data Sheets 107 (12).
- Van der Marck, S.C., Hogenbirk, A., 2003. Criticality results for many benchmark cases: the releases JEFF-3.0, ENDF/B-VI.8, JENDL-3.3, ENDF-B/VII-prelim, and BRC, JEFDOC 974.
- Weigmann, H., et al., 1990. Measurements of ²³⁵U for subthermal neutron energies. In: Proc. Conf. Physics of Reactors: Operation, Design, and Computation, PHYSOR-90, Marseille, France, April 23–26, vol. 3, p. PI 33.
- X-5 Monte Carlo Team, 2003. MCNP – A General Monte Carlo N-Particle Transport Code, Version 5. LA-UR-03-1987.